Jurnal Kejuruteraan 33(2) 2021: 249-255
https://doi.org/10.17576/jkukm-2021-33(2)-10

Simulation Study on the Effect of Dielectrophoresis Force on a Separation of Platelet from Blood Cell in a 3D Mini Channel

Nur Tantiyani Ali Othman* & C. S. Lee
Department of Chemical and Process Engineering,
Faculty of Engineering and Built Environment,
Universiti Kebangsaan Malaysia, 43600, Bangi UKM, Selangor, Malaysia

**Corresponding author: tantiyani@ukm.edu.my*

Received 21 May 2020, Received in revised form 15 September 2020
Accepted 01 October 2020, Available online 30 May 2021

ABSTRACT

In recent years, separation of platelet from a blood cell received growing attention due to its usages for blood disorders or any disease treatment. However, the conventional separation techniques have some constraint due to its limitation to separate the cells with similar properties, costly, requires longer processing time, and less data accuracy. Thus, under the effect of a uniform electric field, a dielectrophoretic (DEP) force was applied as its ability to separate on a similar diameter size of cells, has lower cost, and requires only a small volume of sample. In this study, a 3D mini channel model with a Y-shape was developed using AutoCAD® and the velocity profile distribution was observed using ANSYS© Fluent version 19.1. Three parameters were observed at various an electric field intensity; E=±1 to ±5 V/mm, an electric field frequency, f=1 kHz to 1 MHz and a particle diameter; d=1.3 to 2.0μm. The results show the velocity was increased as the higher of electric field intensity and larger particle diameter. Besides, the DEP force was increased as the higher electric field intensity was charged for all tested frequencies. As well, as the higher the electric field intensity charged and the larger the particle diameter, the stronger of the DEP force. It can be concluded that the DEP force at d=2.0μm and E=5 V/mm was the optimum conditions and obtained the highest result among all the tested parameters. Under these optimum conditions, it shows the DEP force can separate the platelet from the blood cells.

Keywords: Cell platelet, dielectrophoresis; mini channel; separation; ANSYS©; AutoCAD©

INTRODUCTION

In general, human blood consists of a red blood cell, white blood cell, platelet and plasma. These blood cells can be separated to be used in various applications such as for treatment of blood diseases or any organ transplantation. The blood flows in a human body and has three purposes; transporting a gas, nutrients, hormone, heat and waste material throughout a human body. It also plays a crucial role in fighting against pathogens and to control a pH and water balance in the human body (WHO 2002). Also, the platelet has a function of promoting a blood clotting to avoid any blood loss. The platelet has several applications such as used in a common surgery for an organ transplant and trauma patient treatment (Kuhn et al. 2017). Also, blood cells and bone marrow are frequently used in regenerative treatment (Tomlinson et al. 2013). Thus, to fulfill the platelet's demands in a medicine application, a cost involved, material's purity and processing time are among the critical factors in selecting an appropriate separation technique (Hasan et al. 2005). Therefore, the efficacy and the cost-effective of the blood cell separation techniques play a vital role to provide such treatment to cure diseases.

Hitherto, numerous techniques have been reported for the blood cell separation for example, using a centrifugation (Mattanovich et al. 2006), an affinity chromatography acoustic sorting, a fluorescence-activated cell sorting (Md Ali et al. 2016), a magnetic-activated cell sorting (Jung et al. 2018) and a centrifugal elutriation (Buyong et al. 2017; Shahrabi et al. 2018 and Chan et al. 2018). Until now, these techniques shown some constraint and weakness as it is less economic in a large scale and require an enormous amount of a sample to run the separation process as well unable to separate a cell with similar properties, requires a longer time to separate the cell and less data accuracy.

Due to these limitations, an attractive blood cell separation under the influence of non-uniform electric field namely electrophoresis (EP) and dielectrophoresis (DEP) was introduced. This separation technique was preferred in this study as its compatibility to any conductivity solution and able to separate on the similar cells. Since 1950, Professor Pohl was applied to the DEP movement of a neutral particle under the influence of a non-uniform electric field (Pohl et al. 1978 & Pohl et al. 1978). The DEP force was generated to separate cells based on its sizes, and the net electric force will be acted on it to collect and unite the cells.

Generally, the DEP force can be calculated by Equation (1) where d is a cell diameter, ω is an angular frequency, ε is a dielectric constant, $ReK(\omega)$ is a Clausius-Mossotti Factor and ∇E is electric field intensity.

$$F_{dep} = 2\pi\left(\frac{d}{2}\right)^3 \varepsilon_m \mathrm{Re}\left[K(\omega)\right]\nabla E^2 \qquad (1)$$

Furthermore, a design geometry of the mini channel needs to be considered to ensure the well-mixing efficiency will be achieved (Wang et al. 2002). The selection of the design geometry plays a significant factor in the mixing and separation process as it can increase the surface area contact for the ability of the fluids to provide complex molecular diffusion for efficacy well-mixing conditions. Typically, for the mixing and separation purpose, the Y-, T- and serpentine-shape type's channel was often used (Soleymani et al. 2008, Othman et al. 2012, Ait Mouheb et al. 2012, Othman et al. 2013, Milozic et al. 2014, Othman et al. 2015 & Othman et al. 2018). The T-shape type is suitable for multiphase laminar flow regimes in the mixing channel (Soleymani et al. 2008 and Ait Mouheb et al. 2012) and the Y-shape type is shown as the simplest model as it can shorten the mixing time and achieved high mixing efficiency (Wong et al. 2004 & Othman et al. 2015).

Thus, in this study, to observe the separation of the blood cell, a 3-dimensional (3D) mini channel was developed by using Autodesk AutoCAD® 2019 software. Moreover, the effect of DEP forces on the electric field intensity; E, frequency; f and particle diameter; d was studied. These parameters were manipulated to observe the movement of the blood cell under the influence of the DEP force. As well, the particle velocity profile along the mini channel was observed by using ANSYS© software.

METHODOLOGY

A 3D model of the Y-shape mini channel was developed by using Autodesk AutoCAD® version 2019. Then, a simulation studied was conducted on the ANSYS© Fluent version 19.1. Firstly, a set of the study was run as a control set without applying any DEP force on the electrodes. Subsequent, three parameters which are an electric field intensity; E, electric field frequency; f and particle diameter; d are manipulated at E=1-5 V/mm, f=1 kHz-1 MHz and d=1.3-2.0μm to observe a movement of the blood cell in the mini channel as well to determine the effect of the DEP force on the blood cell separation.

DESIGN OF Y-SHAPE MINI CHANNEL MODEL

Figure 1 shows the 2D of the Y-shape mini channel which has five electrodes embedded in it. The mini channel has two inlets, inlet A and B on the left side and two outlets, outlet C and D on the right side. The blood cell was injected into the channel through the inlet A, while the phosphate buffer solution was injected through the inlet B.

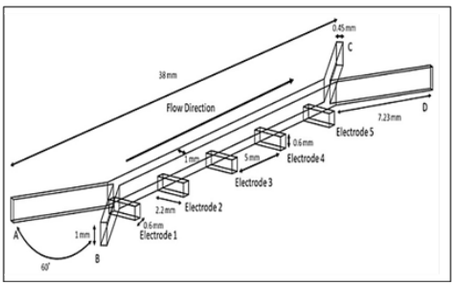

FIGURE 1. 2D Y-shape mini channel.

The angle of between two inlets A and B is set at 30 ° as it will provide better movement of the fluid flow and its interaction once the fluids meet at the Y-junction. It was estimated the platelet in the blood cell flow was flowed out the channel through the outlet C while the other cells will be exit through the outlet D. The length of a mini channel from the inlet to the outlet area is about 38 mm and the distance between the electrodes is 5 mm. The details dimension of the mini channel is shown in Table 1.

TABLE 1. Details dimension of the mini channel (Othman et al. 2013 & Oshii et al. 2014)

Parameter	Value
Total length of channel (mm)	38
Width of channel (mm)	1
Height of channel (mm)	1
Angle of between 2 inlets (°)	30
Length of inlet and outlet (mm)	7.23
Width of inlet and outlet (mm)	0.45
Width and height of electrode (mm)	0.6
Length of electrode (mm)	2.2
Distance of electrodes (mm)	5

MESHING PARAMETERS

In the setting of the ANSYS© Fluent 19.1, there are five types of mesh that can be applied, i.e. tetrahedrons, hexagon dominant, sweep, multizone and Cartesian (ANSYS© Fluent, 2009). The tetrahedron meshing was preferred in this study as it is more suitable for complex geometry. However, the meshing quality is not good enough as it has a low orthogonal quality that can cause an error and affected the accurateness of the simulation work. Thus, the meshing process was improved by using the command '*Inflation*' and '*Body Sizing'*.

DEFINE OF A BOUNDARY CONDITION, MATERIALS AND PARAMETERS

Once the Y-shape mini channel was developed, the boundary condition was defined. The viscosity of the blood cells is

between 3×10^{-3} to 4×10^{-3} Pa. S and the density is 1125 kg/m^3 (Tadepalli et al. 2011). The dielectric constant and conductivity of the blood cell is 73.55×10^3 and 1.23 mho/cm, respectively (Rauf 2013). The phosphate-buffered saline (PBS) was used as a buffer solution to ensure a constant pH; generally, at a pH of 7.4. Typically, the osmolarity and ion concentrations of the solution match with those of the human body. This PBS solution has a density of the 2238 kg/m^3 and a molecule weight of 136.09 kg/kmol (Tadepalli et al. 2011). Three parameters were manipulated with 36 simulations were run at the several ranges of the electric field intensity; E, electric field frequency; f and particle diameter; d as shown in Table 2. The initial velocity of a blood cell and PBS solution was feed through the inlets mini channel at 0.05 m/s.

TABLE 2. Parameters of simulation step up

Value	Intensity, E (V/mm)	Frequency, f (kHz)	Particle diameter, d (μm)
Minimum	± 1	1	1.3
Middle	± 3	10, 100	1.5
Maximum	± 5	1000	2.0

These parameters play an important role to observe the effect of a platelet's movement in the blood flow. The electric field has been generated as there is a difference between the voltages whereas the higher variance will result in the stronger of the electric field intensity. Besides, the electric field intensity is exponential proportional to the DEP force where the higher of the electric field intensity, the stronger of the DEP force. The electric field intensity is defined as some currents changing a flow direction in one seconds. This parameter is linearly comparative to the DEP force as the higher frequency, the stronger of the DEP force where the higher frequency tends to have more energy. The effect on the particle diameter was observed as the larger particle diameter will possess with the greater of the DEP force.

MODEL SELECTION AND GOVERNING EQUATIONS

In the ANSYS© Fluent simulation, three types of a solver model were provided, which are a volume-of-fluid model, mixture model and Eulerian model. The Eulerian model was chosen as it requires less time for running the simulation program (Versteeg & Malalasekera 2007). To solve the numerical method, Equations (2) and (3) are applied that shows continuity and a fluid-fluid momentum equation; respectively where the term of ρ_{rq} is a phase reference density, g is gravitational acceleration, α is a volume fraction, ρ_q is a density of phase q, v_q is a velocity of phase q, v_p is a velocity of phase p, m_{qp} is an interphase mass transfer rate, P is pressure, K_{pq} is an interphase momentum exchange coefficient, v_{qp} is an interphase velocity, τ_q is a q^{th} phase stress-strain tensor, F_q is an external body force, $F_{lift,q}$ is a lift force and $F_{vm,q}$ is a virtual mass force.

$$\frac{1}{\tilde{n}_{rq}}\left(\frac{\partial}{\partial t}\left(\acute{a}_q\tilde{n}_q\right)+\nabla.\left(\acute{a}_q\tilde{n}_q\vec{v}_q\right)=\sum_{p=1}^{n}\left(\dot{m}_{pq}-\dot{m}_{qp}\right)\right) \quad (2)$$

$$\frac{\partial}{\partial t}\left(\acute{a}_q\tilde{n}_q\vec{v}_q\right)+\nabla.\left(\acute{a}_q\tilde{n}_q\vec{v}_q\vec{v}_q\right)= -\acute{a}_q\nabla P_p+\nabla.\bar{\bar{o}}_q+\acute{a}_q\tilde{n}_q\vec{g}+\sum_{p=1}^{n}\left(K_{pq}\left(\vec{V}_p-\vec{V}_q\right)+\dot{m}_{pq}\vec{v}_{pq}-\dot{m}_{qp}\vec{v}_{pq}\right)+\left(\vec{F}_q+\vec{F}_{lift,q}+\vec{F}_{vm,q}\right) \quad (3)$$

RESULT AND DISCUSSION

VELOCITY PROFILE ALONG THE MINI CHANNEL

To ensure the fluid flow in the mini channel is in a laminar condition, the initial inlet flowrate of the blood cell and the PBS solution is set at 0.05, 0.1, 0.15, 0.2, 0.3 and 0.5 m^3/s with the particle size diameter is approximately 1.5 μm. Figure 2 shows the observation of the velocity distribution along the mini channel (left) and at the cross-sectional view of the outlet's area (right). The red contour indicates the maximum flowrate; 0.90 m^3/s, whereas the blue contour indicates the minimum flowrate; 0 m^3/s. The blood cell was injected into the channel through the inlet A while the PBS solution was fed through the inlet B at a similar flowrate. The blood cell flowed out from the channel through the outlet C, while the PBS solution exits through the outlet D.

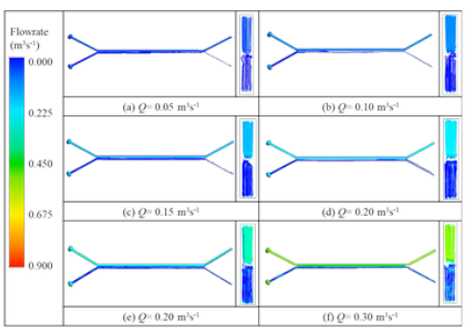

FIGURE 2. Profile of the velocity distribution in the mini channel and at the cross-sectional view of the outlet's area.

The results show as the higher inlet flowrate; Q=0.30 m^3/s, the maximum velocity distribution was observed at both outlets of C and D which is around 0.60 m^3/s. Besides, the side cross-section view showing the velocity distribution of the blood is slightly higher as compared to the PBS solution due to its higher density. It shows the flowrate plays a vital role in cell separation as it may affect the separation's efficiency. Also, the optimum velocity along the mini channel had been achieved at the point where the separation and collection region area occurred.

EFFECT OF DEP FORCE ON A WALL HEAT FLUX

The heat flux has been generated on the surface of the channel wall that is defined as a total heat flux from the conduction and radiation flow. Figure 3 shows the contour of the wall heat flux along the mini channel at several frequencies, f=1-1000 kHz for a particle diameter of d=1.3 µm with the electric field intensity of E=1 V/mm. The red contour represents the maximum value for the wall heat flux which is around 5×10^{-8} W/m^2, while the blue contour represents the minimum value; -7×10^{-8} W/m^2. It was observed the wall heat flux reached the maximum value at the outlet D as the conduction and radiation of the heat flow at that point was the highest value point.

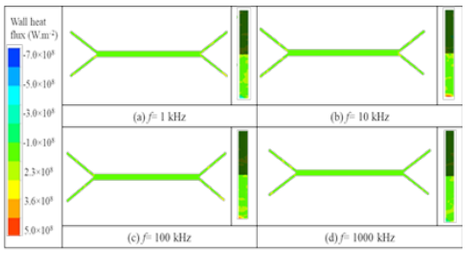

FIGURE 3. Wall Heat Flux at the various frequencies, f (1-1000 kHz) at d=1.3 µm and E=1 V/mm.

Figure 4 shows the effect of the electric field intensity on the channel wall heat flux at various frequencies; f=1 kHz to f=1MHz and at a particle diameter of d=1.3, 1.5 and 2.0 µm. The dotted line represents the data at d=1.3 µm, the dashed line for d=1.5 µm and the solid line for d=2.0 µm. It shows the wall heat flux increases as the electric field intensity was increased and as larger particle size. However, the wall heat flux at the frequency of 100 kHz and 1000 kHz shown a similar result for a particle diameter of d=1.5 and 2.0 µm due to the frequency's effect on the mini channel wall that had reached the maximum level at 100 kHz.

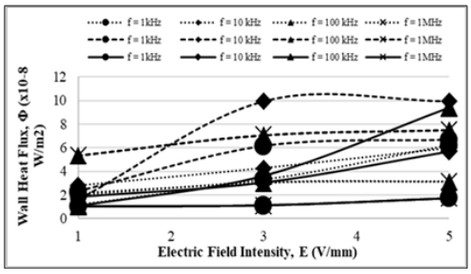

FIGURE 4. The effect of the electric field intensity on the wall heat flux at various of the frequency; f=1 kHz to 1MHz and at particle diameter; d=1.3, 1.5 and 2.0 µm

EFFECT OF DEP FORCE ON PRESSURE

Figure 5 shows the pressure distribution inside the mini channel at various frequencies; f=1-1000 kHz for particle diameter, d=1.3 µm and electric field intensity, E=1 V/mm. The red contour represents the maximum pressure distribution; 1.50×10^{12} Pa, while the blue contour represents the minimum pressure distribution; -2.00×10^{12} Pa. The negative value of the pressure indicates the region is in a vacuum condition. Both of the blood cell and PBS solutions have been injected into the mini channel under low pressure and subsequently, the pressure distribution was increased gradually along the channel till the end of the outlet's area. It shows the pressure in the mini channel for a smaller particle and lower electric field intensity was higher as compared to the larger particle size and higher electric field due to the lower velocity.

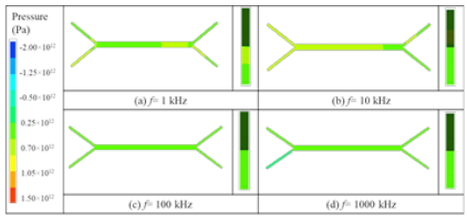

FIGURE 5. Pressure distribution at the various frequencies, f (1-1000 kHz) for particle diameter, d=1.3 µm and electric field intensity, E=1 V/mm

Figure 6 shows the effect of the electric field intensity on the pressure distribution in the mini channel at various frequencies; f=1 kHz to 1MHz and particle diameter of d=1.3, 1.5 and 2.0 µm. The round dotted line represents the data at d=1.3 µm, the dashed line for d=1.5 µm and the solid line for d=2.0 µm. It shows the pressure distribution inside the mini channel decreases as the higher electric field intensity charged on the electrodes since the velocity in the mini channel increases as the electric field intensity increases. It can be explained based on Bernoulli's Principle where the fluid velocity is inversely related to the pressure (Argyropoulos & Markatos, 2015). Thus, the pressure distribution in the mini channel was decreased as the electric field intensity was increased.

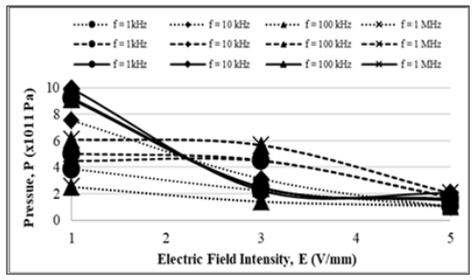

FIGURE 6. The effect of the electric field intensity on the pressure distribution at several of the frequency; f=1 kHz-1MHz and at particle diameter; d=1.3, 1.5 and 2.0 µm.

EFFECT OF DEP FORCE ON A BLOOD CELLS SEPARATION

Figure 7 shows the influence of the electric field intensity; E on the DEP force at the frequencies; f=1 kHz to 1 MHz and at particle diameter of d=1.3, 1.5 and 2.0 µm. The DEP force was calculated by using Equation (1) where

the Clausius–Mossotti factor for frequency was obtained from the previously studied (Sano et al. 2011). It shows the DEP force at the lower frequency; *f*=1 kHz and *f*=10 kHz is in the negative value because of the negativity Clausius-Mossotti factor. Besides, the DEP force is increased as the larger particle size diameter and as the electric field intensity increased. Though, the electric field intensity showed more impact on the DEP force due to the square factor in Equation (1). Therefore, the highest DEP force was obtained at *d*=2.0 µm and *E*=5 V/mm.

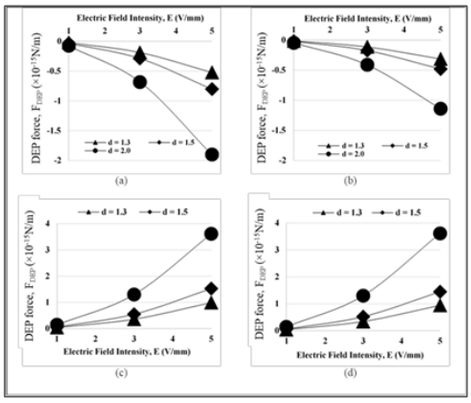

FIGURE 7. The effect of the electric field intensity, *E* on the dielectrophoretic (DEP) force at various of the frequency; *f*=1 kHz-1 MHz with (a) 1 kHz, (b) 10 kHz, (c) 100 kHz and (d) 1000 kHz and at particle diameter; *d*=1.3, 1.5 and 2.0 µm

VALIDATION OF THE RESULTS WITH THE EXPERIMENT DATA

To verify the obtained results, it was compared with the previous experimental work (Oshii et al. 2014) where all the model design, material, parameters and boundary conditions are similar. Figure 8-11 shows the comparison results between the experiment and simulation study on the velocity distribution inside the mini channel on the effect of frequencies; *f*=1 kHz-1MHz, respectively (Figure 8-10), on the effect of the electric field intensities; *E*=1-5 V/mm (Figure 11) and at various particle diameters; *d*=1.3, 1.5 and 2.0 µm. The frequency term with the PS stand for the result of the previous experimental work. The results of the velocity distribution were compared with different particle diameters at *d*=1.3, 1.5 and 2.0µm and the electric field intensity at *E*=3 V/mm.

It showed almost similar relationships and trend patterns between the velocity and electric field where the particle velocity increased as the electric field intensity increases for all tested particle size diameters (Othman et al. 2013 and Othman et al. 2015). Besides that, it was observed the result of the velocity distribution at the frequency of *f*=100 kHz and 1000 kHz are comparable. It proved that the velocity has reached its maximum value at *f*=100 kHz, stable and not increase further at *f*=1000 kHz. However, due to the constraint limitation and has some potential error that occurred during simulation, the inlet velocity on this work was fixed at 0.05 m/s. Thus, some error was shown as compared between this work and Oshii et. al studied which is the error is around 3-40% for the electrical intensity and the error shown up to 80% for the particle diameter.

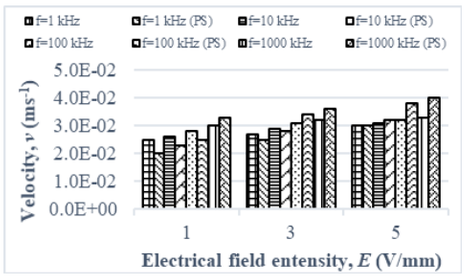

FIGURE 8. Comparison result between experiment (PS) and simulation study on the velocity distribution in the mini channel at frequency; *f*=1 kHz-1MHz, electric field intensity; *E*=1-5 V/mm for particle diameter; *d*=1.3µm

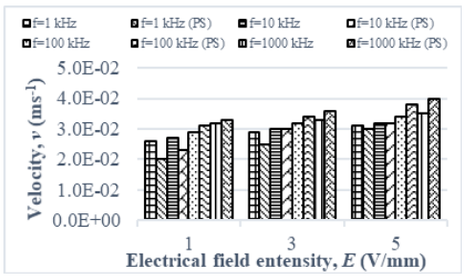

FIGURE 9. Comparison result between experiment (PS) and simulation study on the velocity distribution in the mini channel at frequency; *f*=1 kHz-1MHz, electric field intensity; *E*=1-5 V/mm for particle diameter; *d*=1.5µm

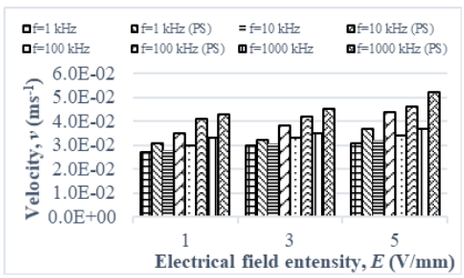

FIGURE 10. Comparison result between experiment (PS) and simulation study on the velocity distribution in the mini channel at frequency; *f*=1 kHz-1MHz, electric field intensity; *E*=1-5 V/mm for particle diameter; *d*=2.0µm

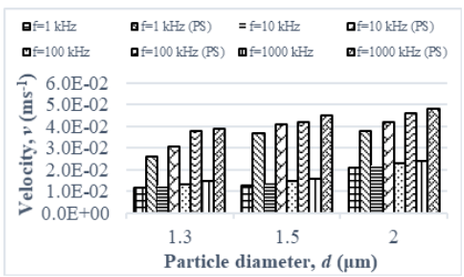

FIGURE 11. Comparison result between experiment (PS) and simulation study on the velocity distribution in the mini channel at frequency; *f*=1 kHz-1MHz, electric field intensity; *E*=3 V/mm and at particle diameter; *d*=1.3, 1.5 and 2.0µm

CONCLUSION

In this study, it shows the velocity was increased with the increasing of the electric field intensity and the size of the particle diameter. Besides, it shows the similar results as compared with the study by Oshii et al. Although the value of the flow velocity was quite different, this study manages to obtain an increasing trend pattern that was comparable with the previous experiment. Also, the DEP force was increased as the higher electric field intensity for all tested frequencies. As well, as the higher the electric field intensity charged and the larger the particle diameter, the stronger of the DEP force has resulted. It can be concluded that the DEP force at d=2.0μm and E=5 V/mm was the optimum condition and obtained the highest result among all the tested parameters.

ACKNOWLEDGMENT

The authors would like to thank Universiti Kebangsaan Malaysia for their financial support under the grant GUP-2017-063.

DECLARATION OF COMPETING INTEREST

None.

REFERENCES

Ait Mouheb, N., Malsch, D., Montillet, A., Solliec, C. & Henkel, T. 2012. Numerical and experimental investigations of mixing in t-shaped and cross-shaped micromixers. *Chemical Engineering Science* 68(1): 278-289.

ANSYS© Fluent 12.0. 2009. User's Guide, ANSYS Inc.

Argyropoulos, C.D. & Markatos, N.C. 2015. Recent advances on the numerical modelling of turbulent flows. *Applied Mathematical Modelling* 39(2): 693-732.

Buyong, M.R., Larki, F., Caille, C.E., Takamura, Y., Hamzah, A.A. & Majlis, B.Y. 2017. Determination of lateral and vertical dielectrophoresis forces using tapered microelectrode array. *Micro & Nano Letters* 13(2): 143–148.

Chan, J.Y., Kayani, A.A., Md Ali, M.A., Kok, C.K., Majlis, B.Y., Hoe, & Marzuki, M. 2018. Dielectrophoresis based microfluidic platforms for cancer diagnostics. *Biomicrofluidics* 12(1).

Hassan, A.A., & Kroll M.H. 2005. Acquired disorders of platelet function. *Hematology Am Soc Hematol Educ Program* 1(51): 403-408.

Jung, O.S., Seo, S.H., Min, H., Kim, M.K., Hahn, B. & Kang, Y.K.J.H. 2018. Magnetic activated cell sorting (MACS) pipette tip for immunomagnetic bacteria separation. *Sensors and Actuators, B: Chemical* 272: 324-330.

Kuhn, V., Diederich, L., Keller, T.C.S., Kramer, C.M. Lückstädt, W., Panknin, C., & Suvorava T. 2017. Red blood cell function and dysfunction: Redox regulation, nitric oxide metabolism. *Anemia, Antioxidants & Redox Signaling* 26(13): 718-742.

Mattanovich, D. & Borth N. 2006. Applications of cell sorting in biotechnology. *Microbial Cell Factories* 5: 1–11.

Md Ali, M.A., Ostrikov, K., Khalid, F.A., Majlis, B.Y. & Kayani, A.A. 2016. Active bioparticle manipulation in microfluidic systems. *RSC Advances* 6(114): 113066-113094.

Miložič, N., Lubej, M., Noval, U., Žnidaršič-Plazl, P. & Plazl, I. 2014. Evaluation of diffusion coefficient determination using a microfluidic device. *Chemical and Biochemical Engineering Quarterly* 28(2): 215-223.

Oshii, K., Choi, J.E. Takei, M. & Hiromichi, O. 2014. Measurement of Dielectrophoretic Velocities of Microparticles in a Minichannel. *Journal of JSEM*, Special Issue (10): 79-84.

Othman, N.T.A., Obara, H.. & Takei, M. 2013. Measurement of fine particles concentration in microchannel using capacitance measurement method. *Japanese Journal of Multiphase Flow* 27(2): 152-159.

Othman, N.T.A., & Takei, M. 2015. Application of electrical capacitance tomography for dense cross-sectional particle migration in a microchannel. *Jurnal Teknologi: Special Issue on Sensor Technology and Control System Applications* 3(17): 85-90.

Othman, N.T.A., & Farid, A.N.M. 2018. Droplets tracing in a T-junction microchannel. *Jurnal Kejuruteraan* 30(1): 47-53.

Pohl H.A. 1978. *Dielectrophoresis: The Behavior of Neutral Matter in Nonuniform Electric Fields*. Cambridge: Cambridge University Press.

Pohl, H.A., Pollock, K. & Crane, J.S. 1978. Dielectrophoretic force: A comparison of theory and experiment. *Journal of Biological Physics* 6(3-4): 133-160.

Rauf A.A. 2013. Dielectric study on human blood and plasma. *International Journal of Science, Environment and Technology* 2(6): 1396-1400.

Sano, M.B., Caldwell, J.L. & Davalos, R.V. 2011. Modeling and development of a low frequency contactless dielectrophoresis (cDEP) platform to sort cancer cells from dilute whole blood samples. *Biosensors and Bioelectronics* 30(1): 13-20.

Shahrabi, S.S., Barzin, J. & Shokrollahi, P. 2018. Blood cell separation by novel PET/PVP blend electrospun membranes. *Polymer Testing* 66: 94-104.

Soleymani, A., Kolehmainen, E., Turunen, I. 2008. Numerical and experimental investigations of liquid mixing in T-type micromixers. *Chemical Engineering Journal* 135: 219-228.

Tadepalli, S.C. Erdemir, A., Cavanagh, P.R. 2011. Comparison of hexahedral and tetrahedral elements in finite element analysis of the foot and footwear. *Journal of Biomechanics* 44(12): 2337-2343.

Tomlinson, M.J., Yang, S. & Kirkham, X.B.J. (2013). Cell separation: Terminology and practical considerations. *Journal of Tissue Engineering* 4, 204173141247269

Versteeg, H. & Malalasekera, W. 2007. *An Introduction to Computational Fluid Dynamics - The Finite Volume Method*. 2nd ed. Pearson-Prentice Hall.

Wang, H., Iovenitti, P., Harvey, E., Masood, S. & Rowan. 2002. Optimizing layout of obstacles for enhanced mixing in microchannels. *Smart Mater Struct* 11: 662-667.

Wong, S., Ward, M. & Wharton, C. 2004. Micro T-mixer as a rapid mixing micromixer. *Sensors and Actuators B:Chemical* 100(3): 359-379.

WHO. 2002. *Establishing a Dialogue on Risks from Electromagnetic Fields*. World Health Organization, Geneva, Switzerland. Geneva.